Journal of Organometallic Chemistry 693 (2008) 2869–2876

Contents lists available at ScienceDirect

Journal of Organometallic Chemistry

journal homepage: www.elsevier.com/locate/jorganchem

Mercury binding by ferrocenoyl peptides with sulfur-containing side chains: Electrochemical, spectroscopic and structural studies

Conor C.G. Scully [a,b], Paul Jensen [a], Peter J. Rutledge [a,*]

[a] School of Chemistry F11, University of Sydney, NSW 2006, Australia
[b] Centre for Synthesis and Chemical Biology, University College Dublin, Belfield, Dublin 4, Ireland

ARTICLE INFO

Article history:
Received 7 December 2007
Received in revised form 28 May 2008
Accepted 2 June 2008
Available online 7 June 2008

Keywords:
Bioorganometallic chemistry
Ferrocene compounds
Mercury
Toxic metal ions
Amino acids
Peptides

ABSTRACT

Ferrocenoyl peptides incorporating amino acids derived from either L-methionine, L-cysteine or DL-homocysteine have been synthesised and investigated as agents for heavy metal binding and detection. Heavy metal–peptide interactions have been characterised using cyclic voltammetry to follow changes in the potential of the Fe(II)/Fe(III) redox couple, revealing that these systems interact with mercury(II) ions more strongly than with other thiophilic heavy metals such as cadmium(II), silver(I) and lead(II). Proton NMR experiments have demonstrated 1:1 peptide:mercury binding and enabled quantitative characterisation of this binding interaction. Crystal structures for two of these ferrocenoyl peptide derivatives have been elucidated, revealing that these compounds adopt a P-1,3′ open solid state conformation in the absence of mercury; this arrangement precludes intramolecular hydrogen bonding between chains, while extensive intermolecular hydrogen bonding is evident. The particular affinity of these systems for mercury(II) opens the possibility of incorporating them in new, biologically inspired sensors for detecting this toxic pollutant.

© 2008 Elsevier B.V. All rights reserved.

1. Introduction

The heavy metals of Group 12 constitute some of the most toxic materials known in Nature [1,2]. Both mercury and cadmium are capable of attacking their respective target organs in humans at very low concentrations, with the kidneys most affected by both elements [1,2]. Without a defense mechanism against them, animal and plant life in locales prone to high levels of cadmium and mercury pollution would be at substantial risk of poisoning by these toxins [3].

Central to biological defense strategies against heavy metal poisoning are sulfur-rich metal-sequestering proteins, metallothioneins (MTs) and phytochelatins (PCs) [4,5]. Sulfur donor atoms are found at the metal-binding sites of many metalloenzymes and proteins, and bind tightly to various soft metal ions [6]. However MTs represent a special subset of sulfur-containing proteins, possessing very high percentages of cysteine residues (up to 30% of the primary structure) [5], much higher than most metal-binding proteins. It is this characteristic that makes MTs effective agents for the sequestration of both mercury(II) and cadmium(II) ions: the numerous sulfur atoms bind these metals tightly, locking them away either permanently or until they can be excreted from the organism.

Because of the high toxicity of mercury and its derivatives, considerable effort has been invested in the development of efficient strategies for their detection [7–9]. Redox-active systems demonstrating excellent sensitivity and high selectivity for mercury over other metals have been reported previously [10–12]. Most of these involve fluorescent or colorimetric techniques, but some electrochemical systems are also known [13].

Ferrocene derivatives have been extensively utilised to study the interactions of chemical hosts with metal ions and other substrates, exploiting the electrochemical properties of the Fe(II)/Fe(III) redox couple [14–18]. The highly reproducible redox behaviour of the ferrocene/ferrocenium redox system enables a range of electrochemical methods, with cyclic voltammetry (CV) most commonly employed [14,16].

In parallel, the bio-organometallic chemistry of ferrocene has attracted considerable attention in recent years, and the literature concerning the preparation and properties of ferrocenoyl peptide derivatives is expanding rapidly [19–22]. However the use of ferrocenoyl peptides in cation sensing applications has received comparatively little attention to date. Kraatz et al. recently utilised ferrocene-containing bioconjugates for the selective detection of various cations including Li(I), K(I), Cs(I), Mg(II) and La(III) [23,17], and in a related study Cheng et al. have prepared a family of ferrocene-linked cyclopseudopeptides and examined their binding properties to alkaline earth metals [24].

Our strategy uses sulfur-containing amino acids and peptides based on the metal-binding motif of MTs in conjunction with the

* Corresponding author. Tel.: +61 2 9351 5020; fax: +61 2 9351 3329.
E-mail address: p.rutledge@chem.usyd.edu.au (P.J. Rutledge).

0022-328X/$ - see front matter © 2008 Elsevier B.V. All rights reserved.
doi:10.1016/j.jorganchem.2008.06.005

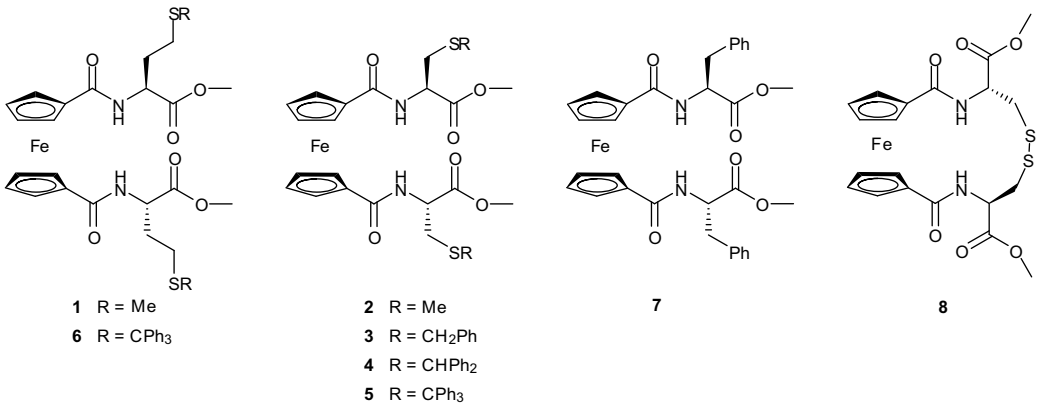

Fig. 1. Ferrocenoyl amino acid derivatives **1**–**8**.

iron(II)/iron(III) redox couple of ferrocene as an electrochemical reporter, to realise new systems for heavy metal recognition and detection. As part of this approach to utilise amino acid and peptide derivatives for sensing heavy metals in a biomimetic context, we report herein the synthesis and metal-binding properties of ferrocenoyl peptides derived from L-methionine, L-cysteine or DL-homocysteine (Fig. 1): the methionine analogue $Fe(C_5H_4–CO–Met–OMe)_2$ (**1**), four thioether derivatives of L-cysteine $Fe(C_5H_4–CO–Cys(Me)–OMe)_2$ (**2**), $Fe(C_5H_4–CO–Cys(Bn)–OMe)_2$ (**3**), $Fe(C_5H_4–CO–Cys(Bzh)–OMe)_2$ (**4**), $Fe(C_5H_4–CO–Cys(Trt)–OMe)_2$ (**5**), and the *S*-tritylhomocysteine compound $Fe(C_5H_4–CO–hCys(Trt)–OMe)_2$ (**6**); we have also tested the L-phenylalanine analogue $Fe(C_5H_4–CO–Phe–OMe)_2$ **7** as a negative control (since this compound lacks the key sulfur atoms) and the cyclic L-cystine derivative **8**.

The results presented here examine the effect of the 'R' group attached to sulfur on the metal-binding affinity of ferrocenoyl peptides **1**–**6**. Four different thioether groups are present in these compounds, with differing steric and electronic properties: methyl, benzyl (CH_2Ph), benzhydryl ($CHPh_2$) and trityl (CPh_3). The corresponding free thiol derivatives were also investigated (c.f. compounds **1** and **2** above, with R = H), as it is the SH group that is responsible for heavy metal binding *in vivo*. However under the conditions used for these binding studies, molecules containing the free thiols bind indiscriminately to transition metal ions and immediately form insoluble precipitates.

Modulating the steric and electronic properties of the sulfur atom using a sulfide in place of the cysteine thiol aids solubility and brings selectivity to interactions of these ferrocenoyl peptides with metal ions: mercury binds to the sulfide derivatives while cadmium, zinc, silver and lead interact weakly or not at all. These interactions have been characterised electrochemically and by NMR. The solid state structures of two representative compounds (the L-methionine and *S*-methyl-L-cysteine compounds **1** and **2**) have also been elucidated.

2. Results and discussion

2.1. Synthesis of ferrocenoyl peptides

Ferrocenoyl peptides **1**–**7** were synthesised from ferrocene-1,1′-dicarboxylic acid **9** and 2 equiv. of the corresponding amino acid methyl ester, coupled using standard peptide coupling methods (Fig. 2) [25]. The cyclic peptide **8** was prepared by coupling ferrocene-1,1′-dicarboxylic acid and L-cystine dimethyl ester at high dilution ($0.001\ mol\ L^{-1}$) and over an extended reaction time (72 h). All compounds were fully characterised. The methionine derivative **1** and the *S*-benzylcysteine compound **3** have previously been reported as part of investigations into the hydrogen bonding properties and helical chirality of ferrocenoyl peptides [26,27], while the phenylalanine analogue **7** [28,29] and cystine derivative **8** [24] have also been synthesised previously.

2.2. Electrochemistry

To probe the metal-binding properties of the ferrocenoyl peptides **1**–**8**, cyclic voltammetry was carried out on these compounds in the presence and absence of the metal ions Hg(II), Cd(II), Zn(II), Pb(II) and Ag(I) in acetonitrile solution. In the 'free' state – i.e. without an additional metal salt present – all of these ferrocene derivatives demonstrate the expected fully reversible one-electron oxidation of Fe(II) to Fe(III) (Table 1). The forward sweep half wave peaks (E_F), reverse sweep half wave peaks (E_R), peak separations (ΔE_P) and half wave potentials ($E_{1/2}$) are summarised in Table 1. The half wave potentials measured for these compounds are in good agreement with those presented elsewhere for such systems [30,31]. Covalently bound amino acids exert an electron withdrawing effect on ferrocene due to the amide bond, which effectively lowers the electron density on the cyclopentadienyl ring making the iron(II) centre more difficult to oxidise; thus the redox poten-

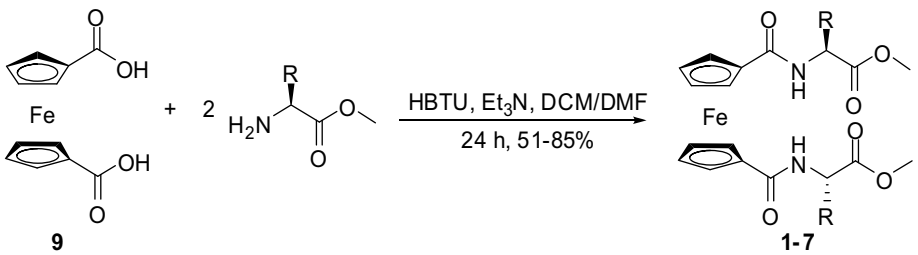

Fig. 2. Synthesis of 1,1′-substituted ferrocenoyl peptides **1**–**7**. Yields: **1** R = CH_2CH_2SMe 51%; **2** R = CH_2SMe 85%; **3** R = CH_2SCH_2Ph 65%; **4** R = CH_2SCHPh_2 77%; **5** R = CH_2SCPh_3 72%; **6** R = $CH_2CH_2SCPh_3$ 73%; **7** R = CH_2Ph 58%. (For the cyclic peptide **8**, starting materials were ferrocene-1,1′-dicarboxylic acid and L-cystine dimethyl ester, reaction time 72 h, yield 29%.)

Table 1
Basic electrochemical properties of 1,1′-substituted ferrocenoyl compounds

Compound	E_F (mV)	E_R (mV)	ΔE_P (mV)	$E_{½}$ (mV)
1	856	795	61	826
2	868	794	74	831
3	861	794	67	828
4	868	800	68	834
5	883	807	76	846
6	870	799	71	835
7	821	758	63	790
8	842	778	64	810

tial is raised relative to ferrocene itself ($E_{1/2}$ = 448 mV versus Ag/Ag^+) [23]. In addition to the electron withdrawing effect of the amide, the amino acid side chain also influences the redox potential of the ferrocene core, as borne out by the observation that compounds **1**–**6** with sulfur-containing residues appended to the cyclopentadiene ring exhibit higher potentials than the phenylalanine derivative **7** which incorporates a non-polar side chain. The through-bond distance between the sulfur and the redox core also effects the redox potential: compare the redox potentials of $Fe(C_5H_4–CO–Met–OMe)_2$ (**1**) (826 mV) vs. $Fe(C_5H_4–CO–Cys(Me)–OMe)_2$ (**2**) (831 mV), or $Fe(C_5H_4–CO–hCys(Trt)–OMe)_2$ (**6**) (835 mV) vs. $Fe(C_5H_4–CO–Cys(Trt)–OMe)_2$ (**5**) (846 mV).

The reversibility of the redox event is indicated by the peak separations: the theoretical peak separation for a diffusion-limited redox event involving the transfer of one electron is 59 mV [32]. In practice, uncompensated resistance exists in the solvent between the reference electrode and the working electrode, so actual values for the peak separation can deviate such that a difference of 10–20 mV above the theoretical value is not uncommon [33]. Of the compounds tested, $Fe(C_5H_4–CO–Met–OMe)_2$ (**1**) has the smallest peak separation at 61 mV and $Fe(C_5H_4–CO–Cys(Trt)–OMe)_2$ (**5**) has the highest at 76 mV; the majority of the values measured deviate by less than 10 mV from the theoretical value.

Complexation of such systems with a cation usually causes a positive shift in the Fe(II)/Fe(III) redox potential, because the positive charge on the adjacent ion inhibits oxidation of the iron centre [14,16]. Upon addition of Hg(II) (as a solution of $Hg(NO_3)_2$ in acetonitrile), the redox potentials of ferrocenoyl peptides **1**, **2**, **3**, **5** and **6** shift to higher potential, with the extent of the shift dependent on the concentration of mercury in the system (Fig. 3 and 4, Table 2). The highest shift in redox potential is shown by $Fe(C_5H_4–Cys(Me)–OMe)_2$ (**2**) which, in the presence of 2 equiv. of Hg(II) changes by 69 mV from the redox potential of the free peptide; the other four compounds exhibit potential changes of between 31 and 47 mV in response to Hg(II). These changes are modest, but are comparable to shifts exhibited by other cation-binding ferrocenoyl peptide systems [17,23]. Each mercury response curve shows a similar plateau effect, with potential changes halting abruptly once between one and 2 equiv. of Hg(II) have been added (reflecting the limited binding capacity of each molecule). Maximum responses for each molecule are summarised in Table 2.

The most striking outcome of this electrochemical analysis is the preference of these compounds for Hg(II) over other metal cations (Fig. 3 and Supplementary material). In contrast to the changes observed in response to Hg(II), compounds **1**, **2**, **3**, **5** and **6** show little or no response to other thiophilic metals such as Cd(II), Zn(II), Pb(II) and Ag(I). Each of these compounds also exhibits some affinity for other metals, but always significantly less than their affinity for Hg(II). For example $Fe(C_5H_4–CO–Cys(Trt)–OMe)_2$ (**5**) shows a small response to Cd(II) and Zn(II), to a total shift of only 5 mV over the same concentration range at which Hg(II) induces a 60 mV shift. $Fe(C_5H_4–CO–Cys(Me)–OMe)_2$ (**2**) undergoes a positive shift of 8 mV in response to Ag(I), and $Fe(C_5H_4–CO–hCys(Trt)–OMe)_2$ (**6**) undergoes a similar shift in response to Cd(II). All other compounds experience only slight perturbations in the presence of other cations tested, none higher than the accepted experimental error of 5 mV. This observation correlates with results reported by Lippolis, who observed that the incorporation of sulfur atoms into a macrocyclic system imparted a similar selectivity for Hg(II) over Cd(II), Pb(II) and Zn(II) [34], and raises interesting possibilities for the development of new, mercury-selective sensor systems based on ferrocenoyl peptides.

In addition to selectivity, a second important factor to consider when discussing the response of these systems to Hg(II) is

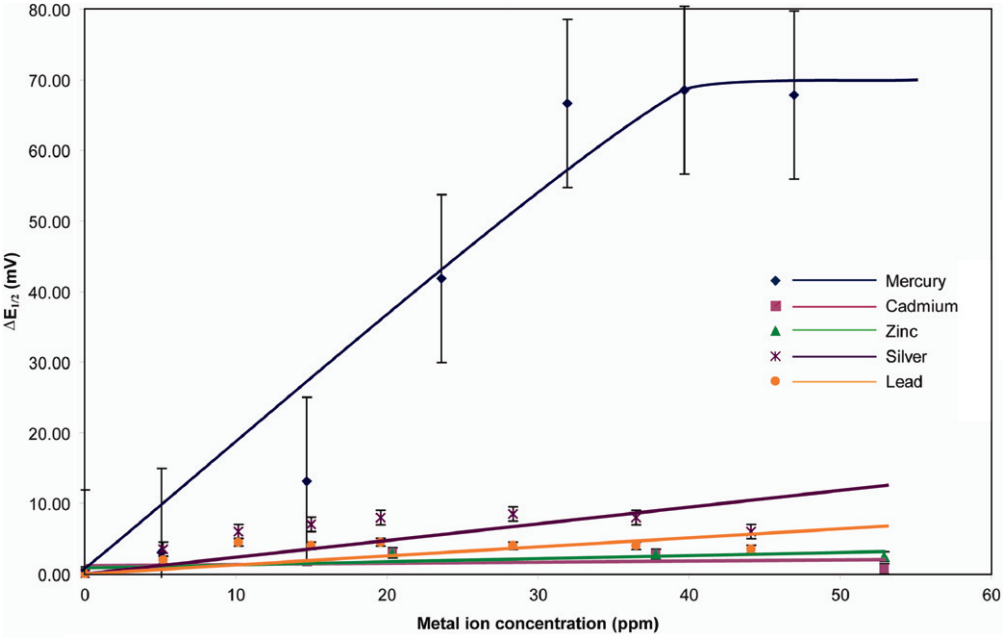

Fig. 3. Titration curves for ferrocenoyl peptide **2** $Fe(C_5H_4–CO–Cys(Me)–OMe)_2$ in response to metal ions Hg(II), Cd(II), Zn(II), Pb(II) and Ag(I), as demonstrated by changes in the potential of the Fe(II)/Fe(III) redox couple in CH_3CN solution. Data points are characterised by *y*-axis standard error bars calculated from the standard error equation in Microsoft EXCEL® and are connected by a trendline based on the points.

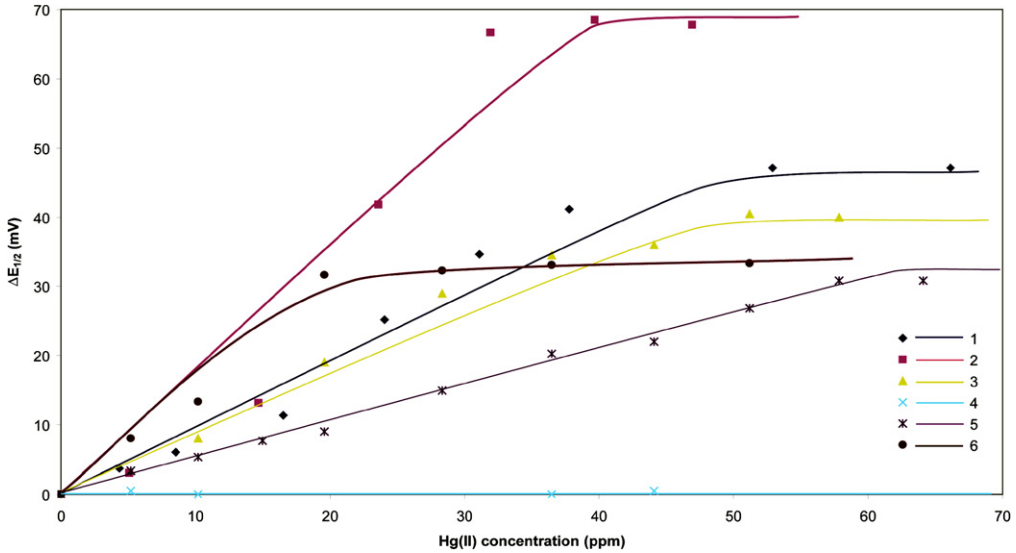

Fig. 4. Activity of *S*-containing ferrocenoyl peptides **1**–**6** in response to mercury, demonstrated by changes in the potential of the Fe(II)/Fe(III) redox couple (all in CH_3CN solution).

sensitivity. This is inherent in how quickly the redox potential changes with respect to increasing mercury concentration, so can be calculated from the slope of the mercury response line. The *S*-methylcysteine analogue $Fe(C_5H_4–CO–Cys(Me)–OMe)_2$ (**2**) is the most sensitive (1.73 mV ppm^{-1}) of these compounds, but the sensitivity we have observed does not come close to the best mercury sensors reported previously [7,8,35,36].

Control experiments were carried out using ferrocene itself and the phenylalanine derivative $Fe(C_5H_4–CO–Phe–OMe)_2$ (**7**), neither of which includes a metal-binding sulfide, to test for interactions between 'non-sulfur' regions of the ferrocenoyl peptide and metal ions. Monitoring the redox potentials of these derivatives upon stepwise addition of mercury(II) nitrate showed both to be unaffected by the heavy metal ions (data not shown), confirming that sulfur–mercury interactions are central to the metal binding observed.

In a less expected result, the cyclic system **8** also demonstrated no discernible redox change upon addition of mercury. This molecule has previously been used to recognise alkaline-earth metals via a binding mode that involves encapsulating the cation via the amide groups [24]. A different mode of interaction was anticipated in the context of heavy metal sensing. It is known that metal ions such as Hg(II) can reduce disulfide bridges in cystinyl peptides [37], and it was anticipated that this could allow the peptide **8** to bind strongly to mercury and respond electrochemically. However it is apparent that this does not occur at the concentrations examined here (0–60 ppm). More surprising again, the *S*-benzhydryl compound $Fe(C_5H_4–CO–Cys(Bzh)–OMe)_2$ **4** also failed to respond to the presence of Hg(II). The reasons behind this are not clear, since both the *S*-benzylcysteine **3** and *S*-tritylcysteine **5** analogues respond to mercury, and the *S*-benzhydryl group would be expected to display properties intermediate between these two (CH_2Ph vs. $CHPh_2$ vs. CPh_3).

Table 2
Hg(II) binding properties of 1,1′-substituted compounds

Compound	Maximum potential shift (mV)	Hg(II) saturation point (ppm)	Sensitivity (mV ppm^{-1})
1	47	53	0.89
2	69	40	1.73
3	40	51	0.78
5	31	58	0.53
6	33	36	0.92

Compounds **4**, **7** and **8** are not shown because no response to mercury was observed for these compounds.

2.3. NMR binding studies

NMR analysis provides further evidence of the interaction between Hg(II) and the sulfur centres in these ferrocenoyl peptides in solution (Fig. 5; NMR binding experiments were carried out in DMSO-d_6 as the mercury–peptide complexes are not sufficiently soluble in CD_3CN at the concentrations required for this analysis). In the absence of mercury, the SCH_3 protons in $Fe(C_5H_4–CO–Met–OMe)_2$ (**1**) resonate at 2.12 ppm (Fig. 5a), while on addition of mercury(II) nitrate, these protons shift downfield, moving to 2.28 ppm with 0.5 equiv. and 2.44 ppm with 1 equiv., a total shift of 0.32 ppm. The methylene protons CH_2SCH_3 exhibit a corresponding perturbation, experiencing a total downfield shift of 0.40 ppm upon complexation. The signals of protons further from sulfur are also affected by metal addition, shifted downfield to a lesser extent as would be expected; for example the amide protons in **1**, four bonds distant from the metal-binding sulfur atoms, move only by 0.10 ppm. In sharp contrast to the changes seen in the presence of Hg(II), the NMR spectrum of **1** does not change discernibly in the presence of Cd(II) or Zn(II), confirming that there is little or no interaction between these metal ions and the peptide. A similar set of NMR results is seen with the *S*-methylcysteine compound **2** (data not shown).

A series of NMR titrations were carried out with compounds **1** and **2**, and changes in the NMR shifts utilised to calculate the association constants of each peptide with Hg(II). Job plots reveal a 1:1 binding stoichiometry in each case (Supplementary material), so the results were analysed as a binary mixture according to the procedure of Hunter et al. [38]. The association constants were calculated to be 21 L mol^{-1} for the L-methionine complex **1** and 25 L mol^{-1} for the *S*-methyl-L-cysteine derivative **2**. These values indicate weak binding (<10^4 L mol^{-1}) [36], which is presumably due primarily to the solvent environment (DMSO-d_6): much stronger interactions (~10^6 L mol^{-1}) between methionine/*S*-methylcysteine and Hg(II) would be expected under aqueous conditions [39,40]. The similar values obtained for the two complexes reflect the similar binding environments in the two peptides.

Table 3
Crystallographic data for **1** and **2**

	$Fe(C_5H_4–CO–Met–OMe)_2$ (**1**)	$Fe(C_5H_4–CO–Cys(Me)–OMe)_2$ (**2**)
Formula of the refinement model	$C_{24}H_{32}FeN_2O_6S_2$	$C_{22}H_{28}FeN_2O_6S_2$
Model molecular weight	564.49	536.43
Crystal system	Triclinic	Orthorhombic
Space group	*P*1 (#1)	$P2_12_12_1$ (#19)
a (Å)	10.003(1)	12.2256(4)
b (Å)	10.547(1)	19.8102(7)
c (Å)	12.536(2)	40.4300(14)
V (Å^3)	1308.1(3)	9791.8(6)
D_{calc} (g cm^{-3})	1.433	1.456
Z	2	16
Crystal colour	Orange	Orange
Crystal habit	Plate	Plate
Crystal size (mm)	0.44 × 0.27 × 0.14	0.29 × 0.27 × 0.08
Temperature (K)	150(2)	150(2)
λ(Mo Kα) (Å)	0.7107	0.7107
μ(Mo Kα) (mm^{-1})	0.777	0.827
T(Gaussian)$_{min,max}$	0.747, 0.905	0.794, 0.936
2θmax (°)	56.62	60
hkl range	−12 13, −13 13, −16 16	−17 17, −27 27, −56 55
N	12488	70809
N_{ind}	10760 (R_{merge} 0.0357)	28136 (R_{merge} 0.0205)
N_{obs}	10083 ($I > 2\sigma(I)$)	25677 ($I > 2\sigma(I)$)
N_{var}	639	1205
Residuals[a] $R_1(F)$, $wR_2(F^2)$	0.0312, 0.0798	0.0328, 0.0777
GoF (all)	1.002	1.04
Residual extrema (e Å^{-3})	−0.245, 0.485	−0.306, 0.650

[a] $R_1 = \Sigma||F_o| - |F_c||/\Sigma|F_o|$ for $F_o > 2\sigma(F_o)$; $wR_2 = (\Sigma w(F_o^2 - F_c^2)^2/\Sigma(wF_c^2)^2)^{1/2}$ all reflections $w = 1/[\sigma^2(F_o^2) + (0.0379P)^2 + 2.4892P]$ where $P = (F_o^2+2F_c^2)/3$.

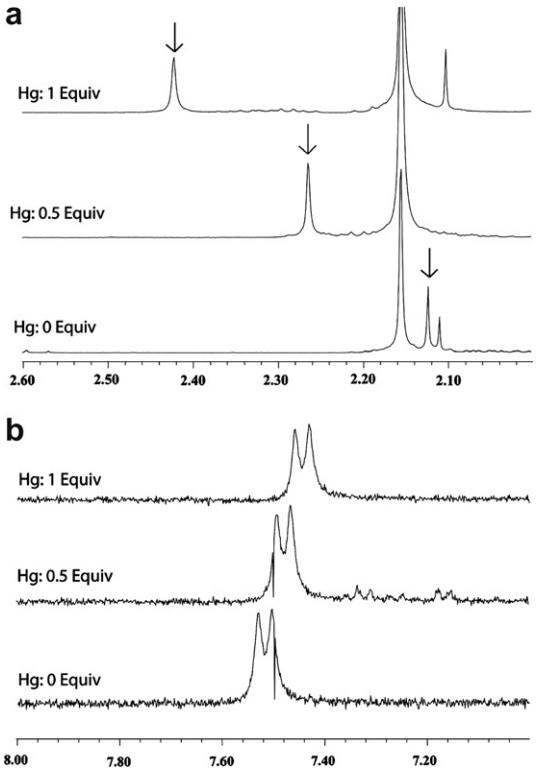

Fig. 5. Change in the 1H NMR spectrum of $Fe(C_5H_4–CO–Met–OMe)_2$ (**1**) induced by the addition of mercury; (a) changes in the position of the SCH_3 proton shift – a move downfield of 0.40 ppm is seen when 1 equiv. of Hg(II) is added; (b) the corresponding change in the amide proton signal, which moves only 0.1 ppm with 1 equiv. of Hg(II).

2.4. X-ray crystallography

X-ray crystal structures were solved for both $Fe(C_5H_4–CO–Met–OMe)_2$ (**1**) and $Fe(C_5H_4–CO–Cys(Me)–OMe)_2$ (**2**) (Table 3 and Fig. 6). Red-orange crystals were obtained by slow diffusion of hexane into a chloroform solution of each ferrocenoyl peptide. Both peptides crystallise in chiral space groups [41]: $Fe(C_5H_4–CO–Met–OMe)_2$ (**1**) crystallises in the *P*1 chiral space group and its asymmetric unit cell contains two independent molecules (only one is shown in Fig. 6 for clarity), while $Fe(C_5H_4–CO–Cys(Me)–OMe)_2$ (**2**) crystallises in the $P2_12_12_1$ space group and its asymmetric unit cell contains four independent molecules (Fig. 6 shows only one for clarity).

The C—C bonds are identical between the two Cp rings of each compound, while the dihedral angles between the ring and the carbonyl double bond show that the amides are co-planer with the ring. The Cp C—C, amide C=O and amide C—N bond distances are all comparable to other ferrocenoyl peptide systems [42]. Both compounds adopt a P-1,3′ open conformation [22] in the solid state, minimising interactions between the two peptide chains on one ferrocene hub. In the P-1,3′ conformation (or 'Xu Conformation'), first reported by Kraatz et al. [43] the substituents on the two Cp rings of one ferrocene moiety are oriented out opposite sides of the sandwich: the angle θ between the peptide chains is 137.5° for **2** and 158.6° for **1**. Such an arrangement precludes intramolecular hydrogen bonding between the chains, however extensive intermolecular hydrogen bonding is evident within the unit cell of both crystals. Hydrogen bonding in molecules of this type has been well studied [42,44,45], and the non-bonding distances between the carbonyl oxygen and amide NH of an adjacent molecule seen in the crystal structures of **1** and **2** (2.86–2.95 Å) are optimal hydrogen bonding distances. This intermolecular hydrogen bonding leads to extended hydrogen-bonded networks in the solid state, in which the amide NH and carbonyl oxygens of adjacent molecules are linked in a head-on fashion.

2.5. Conclusions

In conclusion, we have used a strategy that builds from the metal-binding motif of the MT proteins to design and synthesise a series of simple ferrocenoyl peptide systems which bind mercury more strongly than other metals. The presence of a thioether group at the sulfur atom in the side chain lends these systems a greater affinity for mercury than for other Group 12 metals, silver and lead. Although the sensitivity observed in this study does not rival that seen with the best mercury sensors reported previously [7,8,35,36], the preference of these systems for Hg(II) over other metals opens the possibility of incorporating an *S*-methyl, *S*-benzyl or *S*-trityl binding motif in more responsive contexts to create molecules with high selectivity and sensitivity in detecting this toxic pollutant.

3. Experimental

3.1. Synthesis of ferrocenoyl peptides

Ferrocene-1,1′-dicarboxylic acid was synthesised following the literature procedure [46], as were *S*-methyl-L-cysteine (from L-cysteine using sodium metal and methyl iodide in absolute ethanol [47], *S*-benzyl-L-cysteine (from L-cysteine and benzyl bromide) [48], *S*-benzhydryl-L-cysteine (from L-cysteine and diphenylmethanol in trifluoroacetic acid (TFA)) [49], *S*-trityl-L-cysteine and *S*-trityl-DL-homocysteine (from the free amino acid and

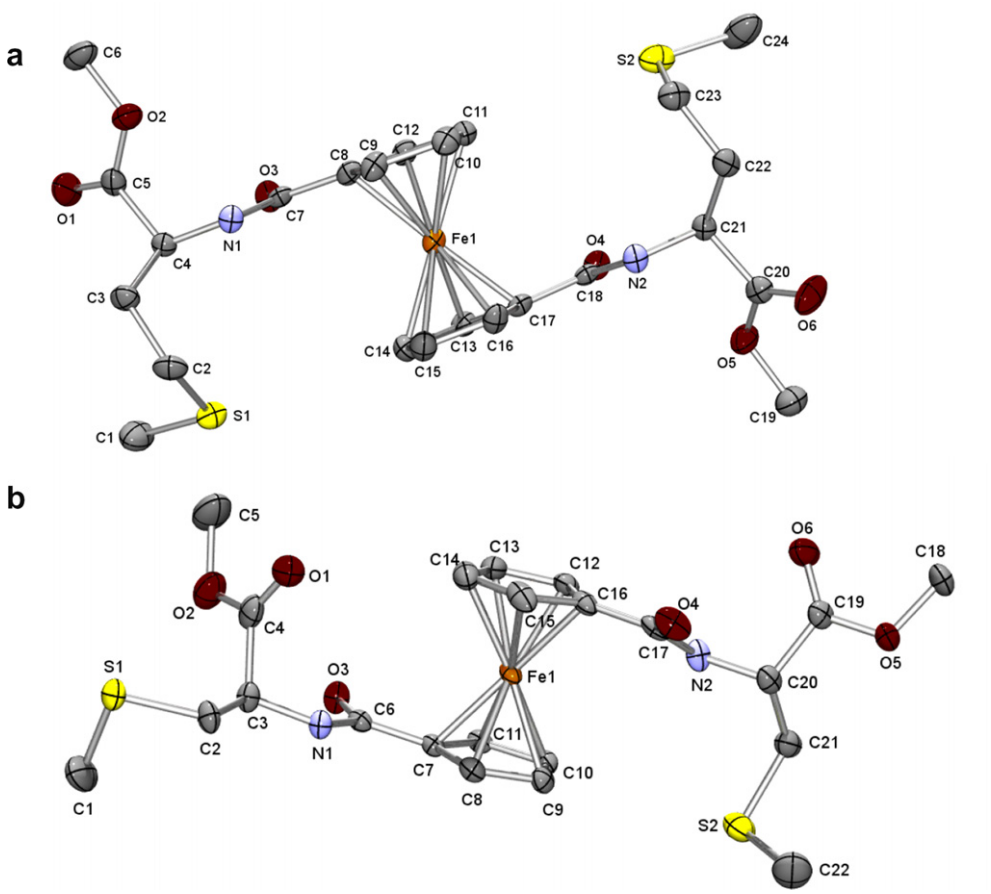

Fig. 6. X-ray crystal structures for the ferrocenoyl peptide derivatives (a) $Fe(C_5H_4–CO–Met–OMe)_2$ (**1**); and (b) $Fe(C_5H_4–CO–Cys(Me)–OMe)_2$ (**2**). Thermal ellipsoids are drawn on the 50% probability level. Hydrogen atoms have been omitted for clarity.

triphenylmethanol in TFA) [50]. *S*-Protected amino acids were converted to their methyl esters in quantitative yield by reaction with thionyl chloride and methanol [51].

Peptide coupling reactions were carried out using the following general procedure [25].

Ferrocene-1,1′-dicarboxylic acid (2.5 mmol) was dissolved in acetonitrile (10 mL) and triethylamine (5.0 mmol) and stirred while *O*-(benzotriazol-1-yl)-*N*,*N*,*N*′,*N*′-tetramethyluronium hexafluorophosphate (HBTU) (5.0 mmol) was added. Stirring was continued for 15 min before the amino acid methyl ester hydrochloride salt (5.0 mmol) was added along with additional triethylamine (5.0 mmol) and stirring continued for 24 h. The reaction mixture was diluted with ethyl acetate (50 mL) to prevent the formation of emulsions and the organic phase was washed with water (50 mL), 1 M HCl (25 mL), water (50 mL), saturated aqueous $NaHCO_3$ (25 mL), water (50 mL) and brine (50 mL), then dried over $MgSO_4$. The solvent was evaporated *in vacuo* to give a brown solid, which was purified by flash chromatography.

3.2. Ferrocenoyl-1,1′-di-L-methionine methyl ester (**1**)

Synthesised according to the general procedure from ferrocene-1,1′-dicarboxylic acid (0.68 g, 2.5 mmol) and L-methionine methyl ester hydrochloride salt (1.00 g, 5.0 mmol). Purified by flash chromatography on silica (Et_2O) to give a bright orange solid (0.97 g, 69%) with data matching those previously reported [26].

3.3. Ferrocenoyl-1,1′-di-S-methyl-L-cysteine methyl ester (**2**)

Synthesised according to the general procedure from ferrocene 1,1′-dicarboxylic acid (0.22 g, 0.80 mmol) and *S*-methyl-L-cysteine methyl ester hydrochloride salt (0.29 g, 1.60 mmol. Purified by flash chromatography on silica (Et_2O) to give a bright orange solid (0.33 g, 77%); R_f 0.33 (Et_2O); m.p. 132–133 °C; δ_H (300 MHz, $CDCl_3$): 2.17 (6H, s, 2 × SCH_3); 2.85 (2H, dd, H_A of ABX, J_{AB} 14.0 Hz, J_{AX} 5.0 Hz, 2 × H_A of CH_2S); 3.02 (2H, dd, H_B of ABX, J_{BA} 14.0 Hz, J_{BX} 9.0 Hz, 2 × H_B of CH_2S); 3.84 (6H, s, 2 × OCH_3); 4.38–4.42 (2H, m, 2 of $Fe(C_5H_4)_2$); 4.53–4.58 (2H, m, 2 of $Fe(C_5H_4)_2$); 4.70–4.74 (2H, m, 2 of $Fe(C_5H_4)_2$); 4.86–4.91 (2H, m, 2 of $Fe(C_5H_4)_2$); 4.98–5.06 (2H, dd, H_X of ABX, J_{XB} 9.0 Hz, J_{XA} 5.0 Hz, 2 × NHCH); 7.57 (2H, d, 2 × NH); δ_C (75.4 MHz, $CDCl_3$): 16.2 (SCH_3); 35.8 (CH_2S); 52.1 (OCH_3); 53.3 (NHCH); 70.6, 71.1, 71.9, 72.3 (8 × CH of $Fe(C_5H_4)_2$); 76.4 (2 × C_{ipso} of $Fe(C_5H_4)_2$); 170.9, 174.1 (4 × C=O); ν_{max} (cm^{-1}, $CHCl_3$): 3377 (m), 2999 (m), 1732 (s), 1647 (s), 1533 (m), 1437 (m), 1194 (s); *m*/*z* (ES+): 559.2 (100%, $[M+Na]^+$), 537.0 (30%, $[MH]^+$); HRMS: found $[M+Na]^+$ 559.0633, $C_{22}H_{28}FeN_2NaO_6S_2$ requires 559.0635.

3.4. Ferrocenoyl-1,1′-di-S-benzyl-L-cysteine methyl ester (**3**)

Synthesised according to the general procedure using ferrocene-1,1′-dicarboxylic acid (0.16 g, 0.58 mmol) and *S*-benzyl-L-cysteine methyl ester hydrochloride (0.30 g, 1.16 mmol). Purified by flash chromatography on silica (EtOAc:hexane, 4:6) to yield an orange oil (0.26 g, 65%) with data matching those previously reported [26].

3.5. Ferrocenoyl-1,1′-di-S-benzhydryl-L-cysteine methyl ester (**4**)

Synthesised according to the general procedure using ferrocene-1,1′-dicarboxylic acid (0.10 g, 0.36 mmol) and *S*-benzhydryl-

L-cysteine methyl ester hydrochloride (0.22 g, 0.72 mmol) to furnish an orange solid (0.23 g, 77%); m.p.: 70–73 °C; δ_H (300 MHz, $CDCl_3$): 2.72 (2 H, dd, H_A of ABX, J_{AX} 5.0 Hz, J_{BA} 14.0 Hz, 2 × H_A of CH_2S), 2.80 (2H, dd, H_B of ABX, J_{BX} 9.0 Hz, J_{AB} 14.0 Hz, 2 × H_B of CH_2S), 3.65 (6 H, s, 2 × OCH_3)), 4.40–4.41 (2H, m, 2 of Fe(C_5H_4)$_2$), 4.56–4.57 (2H, m, 2 of Fe(C_5H_4)$_2$), 4.73–4.74 (2H, m, 2 of Fe(C_5H_4)$_2$), 4.90–4.91 (2H, m, 2 of Fe(C_5H_4)$_2$), 4.98–5.05 (2H, dd, H_X of ABX, J_{XA} 5.0 Hz, J_{XB} 9.0 Hz, 2 × NHC*H*), 5.25 (2H, s, 2 × SC*H*(C_6H_5)$_2$), 7.20–7.43 (20H, m, 2 × (C_6H_5)$_2$); δ_C (75.4 MHz, $CDCl_3$): 33.8 (2 × CH_2S), 52.0 (2 × OCH_3), 53.1 (2 × SCH(C_6H_5)$_2$), 54.0 (2 × NHCH), 70.3, 70.7, 71.6, 72.0 (8 × CH of Fe(C_5H_4)$_2$), 75.6 (2 × C_{ipso} of Fe(C_5H_4)$_2$), 127.3, 127.4, 128.2, 128.4, 128.6 (20 × CH of C_6H_5), 140.5 (4 × C_{ipso} of C_6H_5), 170.2, 173.6 (4 × C=O); ν_{max} (cm^{-1}, $CHCl_3$): 3324 (m), 3012 (w), 1731, 1650 (s), 1527 (m), 1438 (m), 1211 (s); *m*/*z* (ES+): 863 (60%, $[M+Na]^+$), 841 (20%, $[MH]^+$).

3.6. Ferrocenoyl-1,1′-di-S-trityl-L-cysteine methyl ester (**5**)

Synthesised according to the general procedure using ferrocene-1,1′-dicarboxylic acid (0.50 g, 1.82 mmol) and *S*-trityl-L-cysteine methyl ester (1.51 g, 3.65 mmol). Purified by flash chromatography on silica (EtOAc:hexane, 1:1) to yield an orange oil (1.20 g, 72%); δ_H (400 MHz, $CDCl_3$): 2.67 (2H, dd, H_A of ABX, J_{AX} 4.0 Hz, J_{AB} 9.0 Hz, 2 × H_A of CH_2S), 2.80 (2 H, dd, H_B of ABX, J_{BX} 9.0 Hz, J_{AB} 9.0 Hz, 2 × H_B of CH_2S), 3.48 (6H, s, 2 × OCH_3), 4.27–4.28 (2H, m, 2 of Fe(C_5H_4)$_2$), 4.42–4.43 (2H, m, 2 of Fe(C_5H_4)$_2$), 4.66–4.67 (2H, m, 2 of Fe(C_5H_4)$_2$), 4.58–4.69 (2H, m, H_X of ABX, 2 × NHC*H*), 4.76–4.77 (2H, m, 2 of Fe(C_5H_4)$_2$), 7.05–7.42 (30H, m, 2 × (C_6H_5)$_3$); δ_C (100 MHz, $CDCl_3$): 36.8 (2 × CH_2S), 52.0 (2 × OCH_3), 52.9 (2 × NHCH), 67.7 (2 × C(C_6H_5)$_3$), 70.4, 71.0, 71.8, 72.1 (8 × CH of Fe(C_5H_4)$_2$), 76.0 (2 × C_{ipso} of Fe(C_5H_4)$_2$), 126.8, 128.0, 128.2, 127.9, 129.5 (30 × CH of C_6H_5), 144.3 (6 × C_{ipso} of C_6H_5), 170.2, 173.0 (2 × C=O); ν_{max} (cm^{-1}, $CHCl_3$): 1730, 1683 (m), 1506 (m), 1220 (w); *m*/*z* (ES+): 1015 (100%, $[M+Na]^+$); HRMS (ES+): found $[MH]^+$ 993.27039, $C_{58}H_{52}FeN_2O_6S_2$ requires 993.27044.

3.7. Ferrocenoyl-1,1′-di-S-trityl-DL-homocysteine methyl ester (**6**)

Synthesised according to the general procedure using ferrocene-1,1′-dicarboxylic acid (0.04 g, 0.15 mmol) and *S*-trityl-DL-homocysteine methyl ester (0.13 g, 0.30 mmol) to yield an orange oil (0.22 g, 73%); δ_H (400 MHz, $CDCl_3$): 1.16–1.26 (4 H, m, 2 × CH_2CH_2S), 2.16–2.31 (2H, m, 2 × CH_2S), 3.68 (6H, s, 2 × OCH_3), 4.34–4.54 (2H, m, 2 × NHC*H*), 4.56–4.59 (2H, m, 2 of Fe(C_5H_4)$_2$), 4.64–4.68 (2H, m, 2 of Fe(C_5H_4)$_2$), 4.77–4.81 (2H, m, 2 of Fe(C_5H_4)$_2$), 4.87–4.89 (2H, m, 2 of Fe(C_5H_4)$_2$), 7.10–7.42 (30H, m, 2 × (C_6H_5)$_3$); δ_C (75.4 MHz, $CDCl_3$): 29.7 (CH_2CH_2S), 30.5 (CH_2S), 53.0 (OCH_3), 53.5 (NHCH), 70.7, 70.9, 71.6 (8 × CH of Fe(C_5H_4)$_2$), 76.8 (2 × C_{ipso} of Fe(C_5H_4)$_2$) 126.1, 127.1, 127.3, 128.8, 129.3 (30 × CH of C_6H_5), 145.9, 146.9 (6 × C_{ipso} of C_6H_5), 169.8, 172.4 (4 × C=O); ν_{max} (cm^{-1}, $CHCl_3$): 2981 (s), 1737 (m), 1685 (m), 1213 (w); *m*/*z* (ES+): 1044 (100%, $[M+Na]^+$); HRMS (ES+): found $[M+Na]^+$ 1043.28499, $C_{60}H_{56}FeN_2NaO_6S_2$ requires 1043.28366.

3.8. Ferrocenoyl-1,1′-di-L-phenylalanine methyl ester (**7**)

Synthesised according to the general procedure using ferrocene-1,1′-dicarboxylic acid (0.05 g, 0.18 mmol) and L-phenylalanine methyl ester (0.08 g, 0.36 mmol) to afford an orange oil (0.06 g, 58%) which presented data matching those previously reported [29].

3.9. Ferrocenoyl-1,1′-L-cystine dimethyl ester (**8**)

Ferrocene-1,1′-dicarboxylic acid (0.10 g, 0.36 mmol) and HBTU (0.30 g, 0.79 mmol) were dissolved in DMF (1 mL) and triethylamine (0.20 mL, 1.44 mmol) was added. The mixture was diluted with DCM (10 mL) and stirred for 30 min, then diluted with further DCM (250 mL) to give solution A. L-Cystine dimethyl ester dihydrochloride (0.12 g, 0.36 mmol) was dissolved in DMF (1 mL) and diluted with DCM (100 mL). This solution was added dropwise to solution A over 1 h. Stirring was continued for 72 h. The solvent was removed *in vacuo* and the residue redissolved in EtOAc (50 mL) and washed with water (10 mL), 10% citric acid solution (10 mL), water (10 mL), saturated aqueous $NaHCO_3$ (10 mL), water (10 mL) and brine (10 mL), dried ($MgSO_4$) and concentrated *in vacuo* to afford an orange oil. This was purified by flash chromatography on silica (EtOAc:hexane, 1:1) to yield **8** as an orange oil (0.05 g, 29%) with data matching those previously reported [24].

3.10. Cyclic voltammetry

The electrochemical properties of the ferrocenoyl compounds were analysed by cyclic voltammetry [32]. Experiments were carried out at room temperature (22 ± 2 °C) on a BAS-100 potentiostat using a glassy carbon working electrode and a platinum wire auxiliary electrode. The reference electrode was Ag/AgCl (3.0 M NaCl). Titrations were carried out in acetonitrile degassed with argon and the background electrolyte used was 0.1 M tetrabutylammonium perchlorate. All experiments were repeated three times to ensure reproducibility and the working electrode was cleaned between runs by polishing on a microcloth pad with alumina slurry followed by washing with water then acetonitrile. The scan rate was 100 mV s^{-1} in all experiments and iR compensation was applied in all cases. Half wave potentials are reported relative to the Ag/Ag^+ redox potential. Redox potentials are quoted as the half wave potentials ($E_{½}$) and are derived from the formal redox potential ($E^{\circ\prime}$) of the Fe(II)/Fe(III) couple.

3.11. NMR binding studies

Association constants for the binding interactions of **1** and **2** with Hg(II) were calculated according to the method set forward by Hunter and co-workers [38], working in DMSO-d_6 solution as the mercury–peptide complexes are not soluble in CD_3CN at the concentrations required. Thus Job plots for the compounds were constructed (Supplementary material) [52], then two separate 5 mM samples of the peptide and Hg(II) were made up and distributed into ten samples such that the molar ratio (χ) of peptide:Hg(II) varied incrementally from 1.0 to 0.0. The product of the molar ratio and induced shifts ($\Delta\delta$) with respect to the shift for the free ligand was then plotted against the molar ratio.

3.12. X-ray data collection

Both compounds **1** and **2** gave orange crystals in a plate habit. For each, one crystal was attached with Exxon Paratone N to a short length of fibre supported on a thin copper wire inserted in a copper mounting pin, then quenched in a cold nitrogen gas stream from an Oxford Cryosystems Cryostream.

For Fe(C_5H_4–CO–Met–OMe)$_2$ (**1**) a Bruker CCD-1000 area detector diffractometer employing graphite monochromated Mo Kα radiation generated from a fine-focus sealed tube was used for data collection. Cell constants were obtained from a least squares refinement against 8713 reflections located between 4.97° and 56.77° 2θ. Data were collected at 150(2) kelvin with ω scans to 56.62° 2θ. The intensities of 184 standard reflections recollected at the end of the experiment did not change significantly during the data collection.

For Fe(C_5H_4–CO–Cys(Me)–OMe)$_2$ (**2**) a Bruker-Nonius FR591 Kappa APEX II diffractometer employing graphite monochromated Mo Kα radiation generated from a fine-focus rotating anode was

used. Cell constants were obtained from a least squares refinement against 9036 reflections located between 4.40° and 59.87° 2θ. Data were collected at 150(2) kelvin with ω and φ scans to 60.00° 2θ.

The data integration and reduction were undertaken with SAINT and XPREP (Bruker Analytical X-ray Instruments Inc, Madison, Wisconsin, USA, 1995) and subsequent computations were carried out with the XP SHELXTL-Plus graphical user interface (G.M. Sheldrick, Bruker Analytical X-ray Instruments Inc, Madison, Wisconsin, USA, 1995). A Gaussian absorption correction was applied to the data [53]. The $Fe(C_5H_4–CO–Met–OMe)_2$ (**1**) structure was solved in the space group $P1$ (#1), the $Fe(C_5H_4–CO–Cys(Me)–OMe)_2$ (**2**) structure in the space group $P2_12_12_1$ (#19), both by direct methods with SHELXS-97 [54]; each was extended and refined with SHELXL-97 [54]. The non-hydrogen atoms in the asymmetric unit were modeled with anisotropic displacement parameters. A riding atom model with group displacement parameters was used for the hydrogen atoms. The absolute structures were established with the Flack parameter [55,56] refining to −0.004(8) ($Fe(C_5H_4–CO–Met–OMe)_2$, **1**) and 0.002(5) ($Fe(C_5H_4–CO–Cys(Me)–OMe)_2$, **2**).

Acknowledgements

We wish to thank Professor Robert O'Neil (UCD) for help and advice with electrochemistry experiments and Dr Katrina Jolliffe (USyd) for assistance with binding considerations. This work was funded in Ireland by University College Dublin and the Centre for Synthesis and Chemical Biology under the Programme for Research in Third Level Institutions (PRTLI) administered by the HEA, and in Australia by the University of Sydney.

Appendix A. Supplementary material

CCDC 670059 and 670060 contain the supplementary crystallographic data for **1** and **2**. These data can be obtained free of charge from The Cambridge Crystallographic Data Centre via www.ccdc.cam.ac.uk/data_request/cif. Supplementary data associated with this article (full characterisation data for compounds **1**, **3**, **7** and **8**; sample cyclic voltammagrams; titration curves for ferrocenoyl peptides **1**–**6** in response to all metal ions tested; Job plots from NMR binding experiments; and additional crystallographic data for compounds **1** and **2**) can be found, in the online version, at doi:10.1016/j.jorganchem.2008.06.005.

References

[1] A.-M. Florea, D. Büsselberg, BioMetals 19 (2006) 419.
[2] M. Valko, H. Morris, M.T.D. Cronin, Curr. Med. Chem. 12 (2005) 1161.
[3] S. Clemens, Biochimie 88 (2006) 1707.
[4] G. Henkel, B. Krebs, Chem. Rev. 104 (2004) 801.
[5] J.H.R. Kagi, A. Schaffer, Biochemistry 27 (1988) 8509.
[6] W. Kaim, B. Schwederski, Bioinorganic Chemistry: Inorganic Elements in the Chemistry of Life: An Introduction and Guide, John Wiley & Sons, New York, 1994.
[7] C.-C. Huang, Z. Yang, K.-H. Lee, H.-T. Chang, Angew. Chem., Int. Ed. 46 (2007) 6824.
[8] E.M. Nolan, S.J. Lippard, J. Am. Chem. Soc. 129 (2007) 5910.
[9] S.V. Wegner, A. Okesli, P. Chen, C. He, J. Am. Chem. Soc. 129 (2007) 3474.
[10] S.Y. Moon, N.J. Youn, S.M. Park, S.K. Chang, J. Org. Chem. 70 (2005) 2394.
[11] E.M. Nolan, S.J. Lippard, J. Mater. Chem. 15 (2005) 2778.
[12] Z.K. Wu, Y.F. Zhang, J.S. Ma, G.Q. Yang, Inorg. Chem. 45 (2006) 3140.
[13] J.M. Lloris, A. Benito, R. Martinez-Manez, M.E. Padilla-Tosta, T. Pardo, J. Soto, M.J.L. Tendero, Helv. Chim. Acta 81 (1998) 2024.
[14] P.D. Beer, P.A. Gale, G.Z. Chen, Coord. Chem. Rev. 185–186 (1999) 3.
[15] J.D. Carr, S.J. Coles, M.B. Hursthouse, J.H.R. Tucker, J. Organomet. Chem. 637 (2001) 304.
[16] U. Siemeling, T.-C. Auch, Chem. Soc. Rev. 34 (2005) 584.
[17] F.E. Appoh, T.C. Sutherland, H.B. Kraatz, J. Organomet. Chem. 690 (2005) 1209.
[18] C.A. Nijhuis, B.J. Ravoo, J. Huskens, D.N. Reinhoudt, Coord. Chem. Rev. 251 (2007) 1761.
[19] K. Severin, R. Bergs, W. Beck, Angew. Chem., Int. Ed. 37 (1998) 1634.
[20] D.R. van Staveren, N. Metzler-Nolte, Chem. Rev. 104 (2004) 5931.
[21] T. Moriuchi, T. Hirao, Chem. Soc. Rev. 33 (2004) 294.
[22] S.I. Kirin, H.B. Kraatz, N. Metzler-Nolte, Chem. Soc. Rev. 35 (2006) 348.
[23] S. Chowdhury, G. Schatte, H.B. Kraatz, Eur. J. Inorg. Chem. (2006) 988.
[24] H. Huang, L.J. Mu, J.Q. He, J.P. Cheng, J. Org. Chem. 68 (2003) 7605.
[25] S.-Y. Han, Y.-A. Kim, Tetrahedron 60 (2004) 2447.
[26] X. de Hatten, T. Weyhermuller, N. Metzler-Nolte, J. Organomet. Chem. 689 (2004) 4856.
[27] S.I. Kirin, U. Schatzschneider, X. de Hatten, T. Weyhermuller, N. Metzler-Nolte, J. Organomet. Chem. 691 (2006) 3451.
[28] R.S. Herrick, R.M. Jarret, T.P. Curran, D.R. Dragoli, M.B. Flaherty, S.E. Lindyberg, R.A. Slate, L.C. Thornton, Tetrahedron Lett. 37 (1996) 5289.
[29] D.R. van Staveren, T. Weyhermuller, N. Metzler-Nolte, J. Chem. Soc., Dalton Trans. (2003) 210.
[30] M.V. Baker, H.B. Kraatz, J.W. Quail, New J. Chem. 25 (2001) 427.
[31] H.B. Kraatz, J. Inorg. Organomet. Polym Mater. 15 (2005) 83.
[32] A.J. Bard, L.R. Faulkner, Electrochemical Methods: Fundamentals and Applications, 2nd ed., John Wiley & Sons, New York, 2000.
[33] I. Noviandri, K.N. Brown, D.S. Fleming, P.T. Gulyas, P.A. Lay, A.F. Masters, L. Phillips, J. Phys. Chem. B 103 (1999) 6713.
[34] C. Caltagirone, A. Bencini, F. Demartin, F.A. Devillanova, A. Garau, F. Isaia, V. Lippolis, P. Mariani, U. Papke, L. Tei, G. Verani, J. Chem. Soc., Dalton Trans. (2003) 901.
[35] X.J. Zhu, S.T. Fu, W.K. Wong, H.P. Guo, W.Y. Wong, Angew. Chem., Int. Ed. 45 (2006) 3150.
[36] J. Wang, X. Qian, J. Cui, J. Org. Chem. 71 (2006) 4308.
[37] T.W. Greene, P.G.M. Wuts, Protective Groups in Organic Synthesis, 3rd ed., John Wiley & Sons, New York, 1999.
[38] A.P. Bisson, C.A. Hunter, J.C. Morales, K. Young, Chem. Eur. J. 4 (1998) 845.
[39] D. Huljev, M. Dzajo, N. Kristic, P. Strohal, Int. J. Environ. Anal. Chem. 15 (1983) 53.
[40] D.F.S. Natusch, L.J. Porter, J. Chem. Soc., Chem. Commun. (1970) 596.
[41] A. Hess, J. Sehnert, T. Weyhermuller, N. Metzler-Nolte, Inorg. Chem. 39 (2000) 5437.
[42] T. Moriuchi, A. Nomoto, K. Yoshida, A. Ogawa, T. Hirao, J. Am. Chem. Soc. 123 (2001) 68.
[43] Y.M. Xu, P. Saweczko, H.B. Kraatz, J. Organomet. Chem. 637 (2001) 335.
[44] T. Moriuchi, K. Yoshida, T. Hirao, Organometallics 20 (2001) 3101.
[45] T. Moriuchi, A. Nomoto, K. Yoshida, T. Hirao, Organometallics 20 (2001) 1008.
[46] M.D. Rausch, D.J. Ciappenelli, J. Organomet. Chem. 10 (1967) 127.
[47] D.R. Hwang, P. Helquist, M.S. Shekhani, J. Org. Chem. 50 (1985) 1264.
[48] J.M. Yin, C. Pidgeon, Tetrahedron Lett. 38 (1997) 5953.
[49] L. Zervas, I. Photaki, J. Am. Chem. Soc. 84 (1962) 3887.
[50] M. Bodanzky, A. Bodanzky, in: K. Hafner, C.W. Rees, B.M. Trost, J.M. Lehn, P.v.R. Schleyer, R. Zahruchik (Eds.), Reactivity and Structure Concepts in Organic Chemistry, Springer-Verlag, Berlin, 1984.
[51] T.C. McMullen, J. Am. Chem. Soc. 38 (1916) 1228.
[52] J. Kim, B. Raman, K.H. Ahn, J. Org. Chem. 71 (2006) 38.
[53] P. Coppens, L. Leiserowitz, D. Rabinovich, Acta Crystallogr. 18 (1965) 1035.
[54] G.M. Sheldrick, SHELX97 Programs for Crystal Structure Analysis, University of Göttingen, Göttingen, Germany, 1998.
[55] H.D. Flack, Acta Crystallogr., Sect. A 39 (1983) 876.
[56] H.D. Flack, G. Bernardinelli, J. Appl. Crystallogr. 33 (2000) 1143.